Journal of Controlled Release 348 (2022) 431–443

Contents lists available at ScienceDirect

Journal of Controlled Release

journal homepage: www.elsevier.com/locate/jconrel

Contact lenses for pravastatin delivery to eye segments: Design and *in vitro-in vivo* correlations

Ana F. Pereira-da-Mota [a], Maria Vivero-Lopez [a], Maria Serramito [b], Luis Diaz-Gomez [a], Ana Paula Serro [c], Gonzalo Carracedo [b], Fernando Huete-Toral [b], Angel Concheiro [a], Carmen Alvarez-Lorenzo [a,*]

[a] *Departamento de Farmacología, Farmacia y Tecnología Farmacéutica, I+D Farma Group (GI-1645), Facultad de Farmacia, Instituto de Materiales (iMATUS) and Health Research Institute of Santiago de Compostela (IDIS), Universidade de Santiago de Compostela, 15782 Santiago de Compostela, Spain*

[b] *Ocupharm Research Group, Faculty of Optic and Optometry, University Complutense of Madrid, C/Arcos del Jalon 118, 28037 Madrid, Spain*

[c] *Centro de Química Estrutural, Institute of Molecular Sciences and Departamento de Engenharia Química, Instituto Superior Técnico, Universidade de Lisboa, Av. Rovisco Pais, 1049-001 Lisboa, Portugal*

ARTICLE INFO

Keywords:
Drug-eluting contact lenses
Ex vivo permeation studies
In vitro ocular release tests
Ocular biodistribution
In vitro-in vivo correlations

ABSTRACT

Oral administration of cholesterol-lowering statins, HMG-CoA reductase inhibitors, is associated with beneficial effects on eye conditions. This work aims to design contact lenses (CLs) that can sustainedly deliver pravastatin and thus improve the ocular efficacy while avoiding systemic side effects of statins. Bioinspired hydrogels were prepared with monomers that resemble hydrophobic (ethylene glycol phenyl ether methacrylate) and amino (2-aminoethyl methacrylamide hydrochloride) functionalities of the active site of HMG-CoA. Best performing CLs loaded >6 mg/g, *in vitro* fulfilled the release demands for daily wearing, and showed anti-inflammatory activity (lowering TNF-α). High hydrostatic pressure sterilization preserved the stability of both the drug and the hydrogel network. *Ex vivo* tests revealed the ability of pravastatin to accumulate in cornea and sclera and to penetrate through transscleral route. *In vivo* tests (rabbits) confirmed that, compared to eye drops and for the same dose, CLs provided significantly higher pravastatin levels in tear fluid within 1 to 7 h of wearing. Moreover, after 8 h wearing pravastatin was present in cornea, sclera, aqueous humour and vitreous humour. Strong correlations between percentages of drug released *in vitro* and *in vivo* were found. Effects of volume and proteins on release rate and Levy plots were identified.

1. Introduction

Statins are one of the most commonly prescribed drugs in the world. They are orally used for the first line treatment of hypercholesterolemia and reduction of cardiovascular disease risks by inhibiting 3-hydroxy-3-methyl-glutaryl coenzyme A (HMG-CoA) reductase, an important enzyme in the mevalonate pathway. Additionally, a better understanding of the mechanism of action of statins has revealed their pleiotropic capacity [1]. Statins can inhibit the activity of Rho proteins and some of their targets, which provides anti-inflammatory, anti-proliferative, immunomodulatory, neuroprotective, and anti-diabetic effects, among others [2]. Prolonged oral treatments with statins have revealed beneficial effects on ocular health [3]. Statins may promote corneal healing, prevent cataract formation, and also reduce glaucoma severity [3]. Regarding to the posterior segment, oral therapy of hypercholesterolemia with statins has been associated with reduction of hard exudates and microaneurysms in patients with diabetic macular edema, and lower incidence and slower progression of proliferative diabetic retinopathy [4–7].

Diabetes mellitus is one of the world's greatest health challenges and is reaching epidemic proportions [8]. The lack of glycaemia control causes a variety of damages in multiple structures of the anterior and posterior segments of the eye, triggering the development of diabetic keratopathy, dry eye syndrome, cataracts, glaucoma, diabetic retinopathy and macular edema [9,10]. Dysregulation of multiple molecular pathways contributes to upregulation of growth factors and inflammatory cytokines [11,12]. Increased levels of plasma cytokines (tumor necrosis factor-α and interleukin-6) have been found in ocular fluid of diabetic patients [13]. Other inflammatory mediators as prostaglandin E2 may also have a pathogenic role in diabetic retinopathy [14].

* Corresponding author.
E-mail address: carmen.alvarez.lorenzo@usc.es (C. Alvarez-Lorenzo).

https://doi.org/10.1016/j.jconrel.2022.06.001
Received 22 February 2022; Received in revised form 12 May 2022; Accepted 1 June 2022
Available online 13 June 2022

Inhibition of mevalonate pathway by statins reduces oxidative stress, endothelial dysfunction, inflammation, and angiogenesis; thereby improving retina health [15]. Also, statins improve the integrity of endothelial cells, hence preserving the blood–retinal barrier [16]. However, high oral doses may cause adverse systemic collateral effects, mainly on liver and muscle tissue [17]. Therefore, the development of statin ophthalmic formulations that can provide sufficiently high levels of statins in the anterior and posterior segment of the eye, avoiding systemic absorption, may notably improve the ocular outcomes and the overall safety of the treatment. Statin ophthalmic formulations would also be useful for people who do not have hypercholesterolemia.

Pilot studies have shown that topical ocular administration of atorvastatin eye drops is well tolerated in prolonged treatments of dry eye and blepharitis, but frequent instillation is required due to low ocular bioavailability [18]. Sustained drug release from contact lenses (CLs) may provide more prolonged levels in tear fluid and with fewer fluctuations compared to eye drops, which in turn favours drug penetration into anterior eye segment [19–21]. Indeed, the first medicated CL has been approved in 2021 for the management of allergic conjunctivitis [22]. Moreover, it has been recently demonstrated in animal models that such an increase in the amount permeated may make even possible that some specific drugs may reach the posterior segment as recorded for, for example, epalrestat [23], ofloxacin [24] and timolol [25]. Nevertheless, the development of medicated CLs has to face up to the problem of that the affinity of commercially available CLs for most used ophthalmic drugs is low. Therefore, CLs have to be *ad hoc* designed for each target drug in order to uptake therapeutic doses and to provide sustained release on the eye surface [26].

A variety of approaches, which include film coatings, molecular imprinting and drug nanoencapsulation, among others, are under investigation to overcome the loading and release limitations shown by CLs [27–32]. Among these approaches, the recreation of biomimetic receptors that resemble the composition and spatial ordering of the physiological receptor of the drug without compromising relevant optical properties of CLs is pointed out as a successful strategy [26]. Another barrier to be solved for the development and clinical translation of drug-loaded CLs is that *in vitro* release methods that can predict *in vivo* release behaviour are still to be identified because there are too many variables involved [33–36]. In most reports on CLs the *in vitro* release tests are used for optimization of drug release kinetics although with limited basis of how the *in vitro* release profiles may correlate with the *in vivo* release kinetics [37,38].

In a previous study, CLs soaked in atorvastatin calcium solution demonstrated improved drug accumulation *ex vivo* in cornea and sclera, but the drug did not penetrate further probably because its large molecular weight (1155.3 g/mol) and hydrophobicity (Log $P = 6.36$) caused the ocular permeability to be very low [39]. Thus, the present work relied on the hypothesis of that a smaller and more hydrophilic statin, like pravastatin sodium (446.5 g/mol; Log $P = -0.23$ [17]; Fig. 1A), adequately formulated in a CL may get access to deeper eye tissues. Accordingly, the aim of this work was to design CLs bioinspired in the natural receptor of pravastatin, *i.e.*, the HMG-CoA reductase. This natural receptor contains amino acids with a wide variety of hydroxyl groups, hydrophobic groups, and high density of protonated amino groups [40], which could be resembled using 2-hydroxyethyl methacrylate (HEMA), ethylene glycol phenyl ether methacrylate (EGPEM), and N-(3-aminopropyl) methacrylamide hydrochloride (APMA), respectively (Fig. 1). All hydrogels were characterized in terms of solvent uptake, light transmission, mechanical properties and pravastatin loading and release capacity. The effects of high hydrostatic pressure (HHP) and autoclave sterilization on pravastatin solutions and pravastatin-loaded hydrogels were also evaluated. Preliminary screening of cytocompatibility and ocular tolerance was carried out with Balb/3T3 fibroblasts and HET-CAM assay. Pravastatin permeability was assessed *ex vivo* using porcine cornea and sclera tissues. Anti-inflammatory activity of pravastatin-loaded hydrogels was also investigated. Finally, *in vivo* experiments with the most promising CLs were performed in New Zealand white rabbits to investigate the *in vivo* release profiles of pravastatin-loaded CLs and to quantify pravastatin levels in anterior and posterior segment ocular tissues. An additional aim of the work was to identify *in vitro* release conditions that may provide *in vitro-in vivo* correlations (IVIVC). To the best of our knowledge, this is the first time that the effect of the volume and protein composition of the release medium on Levy plots is evaluated.

2. Materials and methods

2.1. Materials

Pravastatin sodium was supplied by Biocon Limited (Bengaluru, Karnataka, India). 2-Hydroxyethyl methacrylate (HEMA) was from Merck (Darmstadt, Germany), and N-(3-aminopropyl) methacrylamide hydrochloride (APMA) from PolySciences Inc. (Warrington, PA, USA). Ethylene glycol dimethacrylate (EGDMA), ethylene glycol phenyl ether methacrylate (EGPEM), 2,2′-azobis(isobutyronitrile) (AIBN), and dichlorodimethylsilane were from Sigma-Aldrich (Steinheim, Germany). Simulated lachrymal fluid (SLF), pH 7.4, was prepared in 1 liter of ultrapure water as follows: 2.18 g $NaHCO_3$ from Probus (Barcelona, Spain), 6.78 g NaCl from Scharlab (Barcelona, Spain), 1.38 g KCl, and 0.084 g $CaCl_2{\cdot}2H_2O$ from Merck (Darmstadt, Germany). Bicarbonate

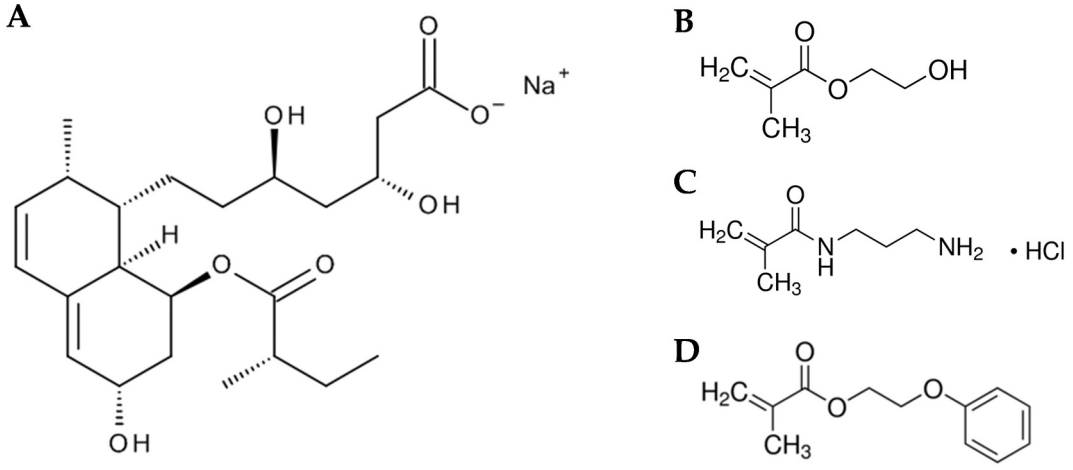

Fig. 1. Molecular structure of pravastatin sodium (A) and monomers used to synthesize the hydrogels: (B) 2-hydroxyethyl methacrylate (HEMA); (C) N-(3-aminopropyl) methacrylamide hydrochloride (APMA); and (D) ethylene glycol phenyl ether methacrylate (EGPEM).

Ringer's solution, pH 7.2, was prepared by mixing 100 mL of buffer solution A (0.071 g KCl, 1.24 g NaCl, 0.49 g $NaHCO_3$, and 0.02 g NaH_2PO_4, from Merck (Darmstadt, Germany)) and buffer solution B (0.031 g $MgCl_2$, and 0.023 g $CaCl_2$ from Panreac (Barcelona, Spain)). Ultrapure water (resistivity >18.2 MΩ cm; Milli-Q®, Millipore Ibérica, Madrid, Spain) was obtained by reverse osmosis. Methanol 99.9% for LC-MS grade was from Fisher Scientific (Loughborough, UK). Acetonitrile for HPLC LC-MS grade and NaOH were from VWR Chemicals (Fontenary-Sous-Bois, France). Balb/3T3 fibroblasts (ATCC CCL-163™) and THP-1 cells (ATCC TIB-202™) were provided by American Type Culture Collection (ATCC, Manassas, VA, USA). Dulbecco's modified Eagle medium (DMEM), Dulbecco's phosphate buffered solution (DPBS), and RPMI 1640 was from Fisher Scientific (Newington, NH, USA). Fetal bovine serum, antibiotic solution (penicillin and streptomycin), lipopolysaccharides (LPS) from *Escherichia coli* O111:B4, phorbol 12-myristate 13-acetate (PMA), and TrypLE® were acquired from Sigma-Aldrich (St. Louis, MO, USA). Cell counting kit-8 (CCK-8) was from Dojindo Molecular Technologies (Rockville, MD, USA). Schirmer test strips were from Contacare Ophthalmics and Diagnostics (Gujarat, India). Pentobarbital (400 mg/mL) was from Richter Pharma AG, Wels, Austria.

2.2. Synthesis of hydrogel discs and CLs

Four different hydrogels were synthesized combining HEMA, EGPEM, and APMA, as summarized in Table 1. Briefly, the monomers were mixed into glass vials and magnetically stirred (200 rpm) for 120 min at room temperature. Then, EGDMA (crosslinker) and AIBN (initiator) were added, and the solutions were magnetically stirred again (100 rpm) for 10 min. The resulting solutions were immediately injected into moulds composed of two glass plates (10 × 10 cm) separated by a silicone frame with 0.3 mm of thickness, and heated at 50 °C for 12 h, and then to 70 °C for further 24 h for thermal polymerization [41].

After polymerization, each hydrogel sheet was boiled (1 L water) for 15 min to remove unreacted substances and facilitate cutting in the form of 10-mm discs. The discs were alternatively washed in water and 0.9% NaCl twice a day (200 rpm magnetic stirring, room temperature), until complete removal of the unreacted monomers as monitored spectrophotometrically (UV–Vis spectrophotometer, Agilent 8453, Waldbronn, Germany). Finally, the discs were dried at 70 °C for 24 h before being stored and used in further experiments.

CLs were prepared with the same composition as E200A40 hydrogel, but adding more AIBN (14.79 mg, initiator) for a complete polymerization of the thinner hydrogels. The monomer solution was pipetted (60 μL) in curved polypropylene moulds (similar to those used for industrial production of CLs) to have final CL dimensions in the hydrated state (phosphate buffer pH 7.4) of approx. 12 mm diameter, 7.8 mm curvature, and 0.1 mm thickness. After polymerization at 50 °C for 12 h and then at 70 °C for 24 h, all CLs were washed as described above. Finally, the CLs were dried at 70 °C for 24 h.

2.3. Hydrogel characterization

Solvent uptake capacity was evaluated, in triplicate, from the mass increase of previously weighed dried discs (W_0) after being immersed in 10 mL of SLF at room temperature without agitation until equilibrium (W_t), as follows:

$$\text{Solvent } uptake\ (\%) = [(W_t - W_0)/W_0] \times 100 \quad (1)$$

Water contact angles on dried and wet hydrogels (10 mm in diameter) were measured using the sessile drop method with a Phoenix-300 goniometer (Surface Electro Optics Co., Suwon, Korea). The measurements were performed over 2 discs of each formulation, at room temperature, and with distilled water. A total of 10 images were captured in 10 s, and the best-adjusted pictures were selected to obtain the contact angle value.

Ion permeability was recorded in triplicate by fixing individual wet hydrogel discs between two flat Teflon washers (8 mm open diameter), which were fixed in a screw cap (open top) and screwed in a 5-mL HPLC vial. The bottom of the vials was previously removed. The vials were placed downward in beakers containing 15 mL distilled water at 35 °C and magnetically stirred (130 rpm) (Fig. S1 in Supplementary Material). The surface available for diffusion was 50.27 mm^2. Then 4 mL NaCl 0.1 M solution were added to the vial and the conductivity was recorded as a function of time using an InLab® 741 conductivity probe fitted to a Mettler Toledo T70 titrator (Greifensee, Switzerland).

The transmittance of the hydrogels swollen in SLF was recorded in an UV–Vis spectrophotometer (Agilent 8453, Waldbronn, Germany), in the 200–800 nm range ($n = 3$). Mechanical properties of dog bone-shaped hydrogels (18 × 5 mm, in the center 6 × 2.5 mm) were tested using a TA.XT Express Texture Analyzer (Stable Micro Systems, Godalming, UK) fitted with a 50 N load cell. The hydrogel probes ($n = 5$) were fixed to the upper and lower clamps, and the tensile test was carried out applying a test speed of 0.25 mm/s and 0.005 N trigger force. The elastic modulus was calculated from the initial slope of the engineered stress-strain curve [42].

2.4. Pravastatin loading and release

Pravastatin was loaded by soaking the dried discs in pravastatin sodium (0.1 mg/mL; 10 mL) solution. The experiment was repeated several times and in each run 4 discs of each composition were tested. The vials were kept under oscillatory movement (180 osc/min) at room temperature and protected from light. After 48 h, the absorbance of the loading solution was measured at 238 nm (UV–Vis spectrophotometer, Agilent 8453, Waldbronn, Germany). The amount loaded was calculated as the difference between the initial and final amount of pravastatin in the solutions using previously prepared calibration curves. The network/water partition coefficient was estimated as follows [43]:

$$K_{N/W} = \left[\text{Loading} - \left(V_s/W_p\right) \times C_0\right]/C_0 \quad (2)$$

In this equation, V_s is the solvent volume sorbed by the hydrogel, W_p the dried hydrogel weight, and C_0 the initial concentration of the loading solution.

In vitro drug release patterns were recorded by immersing loaded discs ($n = 4$) in vials containing 10 mL of SLF (pH = 7.4) at 37 °C. The discs were previously rinsed with SLF to remove the excess of pravastatin from the hydrogel surface. The experiments were performed for 120 h under oscillatory movement (180 osc/min) and protected from light. At predetermined time points, 3 mL of the release medium were collected, absorbance measured at 238 nm and the sample returned to the vial immediately. After 8 h of experiment, 2 mL of the release medium were collected and replaced by the same volume of fresh SLF to avoid false plateaus. The test was carried out under sink conditions.

2.4.1. Pravastatin release from sterile CLs

The synthetized CLs (E200A40 composition) were immersed in a pravastatin solution (0.1 mg/mL) for 48 h and then sterilized in closed packages by high hydrostatic pressure (HHP) (see Section 2.8). The CLs were stored at room temperature until release experiments were performed. The CLs were immersed in 2 or 10 mL of SLF without or with lysozyme or bovine serum albumin (2.68 mg/mL). The experiments

Table 1
Composition of the monomer mixtures used to synthesize the hydrogels. To each mixture, 4.93 mg AIBN were added.

Hydrogel code	HEMA (mL)	EGDMA (μL)	EGPEM (μL)	APMA (mg)
E0A0	3	12.10	–	–
E200A0	3	12.10	112.50	–
E200A40	3	12.10	112.50	21.45
E0A40	3	12.10	–	21.45

were performed at 37 °C, under oscillatory movement (180 osc/min) and at predefined timepoints, 150 μL were removed and replaced by the same volume of fresh SLF, or SLF plus lysozyme or BSA. The amount of pravastatin released from the CLs was quantified by HPLC (as described in section 2.7) after denaturation of the proteins (section 2.9.2). The amount of protein deposited on blank (non-drug loaded) CLs was monitored at 280 nm (UV–Vis spectrophotometer, Agilent 8453, Waldbronn, Germany) at the same time points as for the drug release test.

2.5. HET-CAM test

The potential ocular irritation of pravastatin-loaded hydrogels was evaluated using the hen's egg test on the chorioallantoic membrane (HET–CAM) assay, as previously described [44]. On the eighth day after egg fertilization, the eggshell at the wider extreme of the egg was removed and the CAM was exposed. Pravastatin-loaded hydrogels (n = 2, 10 mm discs) and 300 μL of pravastatin solution (0.1 mg/mL) were carefully placed on the CAM and the possible haemorrhage, vascular lysis, or coagulation of the vessels was monitored for 5 min. 0.9% NaCl and 0.1 N NaOH solutions were used as negative and positive controls, respectively. Finally, the irritation score (IS) was calculated as reported previously [44].

2.6. Cytocompatibility and anti-inflammatory activity

Balb/3T3 fibroblasts (ATCC CCL-163™) were cultured in Dulbecco's modified Eagle medium (DMEM) with 10% fetal bovine serum and 1% antibiotics (10,000 U/mL penicillin and 10,000 μg/mL streptomycin) at 37 °C and 5% CO_2. Then, cells were detached from the culturing flasks using TrypLE® at 80% confluence. Suspended cells were counted, seeded in wells of 96-well plates (20,000 cells/well), and allowed to attach for 24 h.

Non-loaded and pravastatin-loaded hydrogels were evaluated. Dried hydrogels (10 mm discs) were immersed in pravastatin solution (0.1 mg/mL) for 48 h or in 0.9% NaCl (non-loaded hydrogels), cut in four symmetric pieces and sterilized using HHP method (described in Section 2.8.). One piece of each hydrogel was placed in contact with the cells and incubated for 24 or 48 h. Five replicates for each hydrogel were tested. Cells without treatment (negative control) and cells incubated with pravastatin solution (0.05 and 0.1 mg/mL) were also tested.

Cell viability was assessed using a Cell Counting kit-8 (CCK-8) following the manufacturer' instructions. Briefly, hydrogel pieces and culture medium were removed from the wells, and 200 μL of a CCK-8 working solution (10% *v/v* CCK-8 reagent in DMEM) were added to each well and incubated for 1 h at 37 °C. The absorbance was measured at 450 nm (UV Bio-Rad Model 680 microplate reader, Hercules, CA, USA), and cell viability (%) was normalized to the negative control as follows.

$$\text{Cell } \textit{viability}\ (\%) = \left(\text{Abs}_{\text{exp}} / \text{Abs}_{\text{negative } \textit{control}}\right) \times 100 \quad (3)$$

The anti-inflammatory effects of non-loaded and pravastatin-loaded E200A40 hydrogels were evaluated in THP-1 human monocytes (ATCC TIB-202™). The macrophage cell line was cultured in RPMI 1640 supplemented with 10% fetal bovine serum, 1% penicillin-streptomycin and maintained at 37 °C, 5% of CO_2 and 90% relative humidity. Phorbol 12-myristate 13-acetate (PMA; 200 nM) was added to promote the differentiation of THP-1 cells into macrophages incubating for 72 h at 37 °C [45]. After macrophage differentiation, PMA solution was removed and cell monolayers were washed with DPBS, trypsinized and a specific cell scraper was used to remove all adherent cells. Macrophages were seeded at a density of 50,000 cells/well into 24-well plates for 6 h. After this period, one piece of non-loaded and loaded E200A40 previously sterilized discs was added to each well. Also, three different concentrations of pravastatin sodium (0.1, 1, and 10 μM) were tested. After 12 h, cells were stimulated with LPS (100 ng/mL) and incubated for 24 h at 37 °C, 5% of CO_2 and 90% relative humidity. Cells treated with only LPS served as positive controls, while unstimulated cells (without LPS) were used as negative controls. After incubation, cell culture supernatants were collected, and the secretion of TNF-α and IL-6 was analyzed by specific ELISA kits (Sigma-Aldrich, St. Louis, MO, USA, and RayBiotech, Norcross, GA, USA, respectively) following the manufacturer's instructions.

2.7. Ex vivo cornea and sclera permeability

Ex vivo cornea and sclera permeability assays were carried out with pravastatin-loaded E200A40 and E0A40 hydrogels according to previous described protocols [44,46]. Fresh porcine eyes were provided by a local slaughterhouse and transported completely immersed in PBS solution in an ice bath. Corneas and sclera tissues were isolated, washed with PBS, and mounted in vertical diffusion Franz cells. Both chambers were filled with bicarbonate Ringer's solution, pH 7.2, prepared with concentrations of bicarbonate and electrolyte ions similar to those in the extracellular fluid [47] and commonly used to preserve ocular tissues [48]. The receptor chamber was immersed in a water bath at 37 °C. After 30 min of tissues balance, the buffer solution in the donor chamber was removed and replaced with pravastatin-loaded hydrogels (E200A40 and E0A40) or 1 mL of pravastatin solution (128 μg/mL). SLF (2 mL) was added onto the hydrogels, and the donor chambers were covered with parafilm to prevent evaporation. Samples (1 mL) from the receptor medium were taken at 30 min, 1, 2, 3, 4, 5 and 6 h and replaced with the same volume of fresh bicarbonate Ringer's solution. After 6 h of experiment, the corneal and scleral tissues were removed from the diffusion cells, and soaked in 3 mL of ethanol:water (50:50 *v/v*) mixture overnight at 37 °C under magnetic stirring. Then, they were sonicated for 99 min at 37 °C and centrifuged (1,000 rpm, 5 min, 25 °C), and the supernatants filtered and centrifuged again (14,000 rpm, 20 min, 25 °C) for HPLC analysis.

The amounts of pravastatin in the donor chamber, drug accumulated in the tissues and drug permeated were quantified by HPLC (AS-4140 autosampler, PU-4180 pump, LC-NetII/ADC interface box, CO-4060 column oven, MD-4010 photodiode array detector, JASCO, Tokyo, Japan) fitted with a Waters Symmetry C18 column (5 μm, 3.9 × 150 mm) and operated with ChromNAV software v.2. Mobile phase consisted of methanol:0.02 M sodium phosphate (NaH_2PO_4) buffer (50:50 *v/v*, pH adjusted to 7.0 with NaOH) at 1.00 mL/min and 25 °C [49]. The injection volume was 50 μL, and the total run time of each sample was 10 min. Pravastatin was quantified at 238 nm (retention time 5.15 min). The HPLC method was validated using pravastatin solutions in bicarbonate Ringer's buffer in the 0.05 to 16 μg/mL range. The flux, J, was obtained from the slope of the regression of the amount of drug in the receptor chamber (Q) per surface area available for diffusion *versus* time (t) [50,51]. The apparent permeability coefficient, P_{app}, was calculated as the ratio between the flux (J) and the drug concentration in the donor chamber measured at time point 6 h.

2.8. Sterilization and stability of pravastatin-loaded hydrogels

The stability of pravastatin-loaded E200A40 and E0A40 hydrogels after sterilization was evaluated using two different protocols: a) steam heat (SH; autoclave Uniclave 88/75 L; A. J. Costa, Cacém, Portugal) for 1 h at 1 bar and 121 °C sterilization; and b) high hydrostatic pressure (HHP; 70 °C, 600 MPa for 10 min) sterilization. Previously developed protocols were followed [39]. After sterilization, the amount of pravastatin in the hydrogels and the release kinetics were monitored again as described above (Section 2.4).

Aliquots of pravastatin solution (0.1 mg/mL) were also sterilized by SH or HHP under the same conditions as the hydrogels and investigated regarding degradation products using HPLC (Section 2.7).

Additionally, stability of pravastatin during exposition to daylight conditions was evaluated by exposing aliquots of pravastatin aqueous

solution (0.05 mg/mL) in quartz cells to fluorescent tube light (F8T5 Daylight, 6500 K, Hitachi, Japan) for 6 h at room temperature. HPLC chromatograms were recorded before and after the exposition to the light (Section 2.7).

2.9. *In vivo* experiments: Drug release and tissue accumulation

Dried CLs were individually packed in polyamide/polyethylene bags filled with 10 mL of pravastatin solution (0.1 mg/mL). The CLs were maintained for 48 h in pravastatin solution, sterilized by HHP and stored at room temperature until being placed on the rabbits ocular surface. All experiments were performed according to the Association for Research in Vision and Ophthalmology Statement for the Use of Animals in Ophthalmic and Vision Research and to European Directive 2010/63/EU. The protocols were approved by the Committee for Animal Experimentation of the Universidad Complutense de Madrid [Registration number: O00023280e2100023620].

Ten healthy male New Zealand white rabbits (age approx. 3 months weighing 4.36 ± 0.23 Kg) were included in the *in vivo* experiments. The animals were in a light-controlled room (12 h light/ 12 h dark cycles) at 18 °C in individual cages with total access to food and water. Rabbits with low weight or corneal disruptions were not included in the study. During the experiments and sampling, the rabbits were placed in rabbit restrainers with continuously monitoring to not remove the CLs placed on the ocular surface.

The rabbits were randomly divided into two groups, CLs group (n = 6) and one-eye drop group (n = 4). In the eye drops group, one drop (50 μL; 2 mg/mL of pravastatin) was instilled and the rabbits were euthanized 8 h after. The CLs group was divided into other two subgroups, the subgroup of rabbits (n = 3) that wore the CLs for 8 h and were euthanized after this period, and the subgroup of rabbits (n = 3) that wore the CLs for 10 h and were euthanized after 24 h (summarized in Fig. 2). No confounders were controlled as the presence of the CLs was evident on the ocular surface of the rabbits.

For the sample size calculation, the 3R's principles were followed minimizing the number of rabbits used and trying to obtain the most reliable results. A total of 10 animals were used in this two-treatment parallel-design study. This design allowed the study detected a treatment difference at 0.05 significance level with a probability of 80% if the difference between treatments was 2.03 times the standard deviation.

2.9.1. *In vivo release*

The ocular surface of each rabbit was carefully inspected with a VX75 slit lamp (Luneau Technology, Chartres, France) before and after 8 h of the experiment. The CLs were removed from the sterilized bags, rinsed with sterile saline solution for CLs (to remove excess drug on the surface of the CL), and carefully placed on the rabbit right eye without local anaesthesia. The CLs were placed in the cornea and bulbar conjunctiva below the nictitating membrane. No nictitating membranectomy or tarsorrhaphy was needed. To prevent drying of CL on the surface of the eye, every 15 min the rabbits' eyes were closed for 1 min. The left eye was kept as control without treatment. In the eye drop group, a single drop (50 μL) of 2 mg/mL of pravastatin solution, which contained the same amount of pravastatin as that released from the CLs after 8–10 h, was gently instilled in the lower conjunctival sac of the right eye using a micropipette. Before and after administration (t = 5 min, 15 min, 30 min, and every hour until 8 or 10 h) tear fluid samples were collected using Schirmer test strips which were placed in the tarsal conjunctiva of the lower lid for 10 s with closed eyes [52]. The volume of tears collected from the Schirmer strips was recorded as millimetres of moistened strip. The mean residence time (MRT) was calculated as the area under the curve of concentration x time *versus* time (AUMC) referred to the area under the curve of concentration *versus* time (AUC). Both AUMC and AUC were calculated from the experimental data applying the trapezoidal rule [53]. After wearing, CLs were extracted with SLF (0.8 mL under stirring at 37 °C for 24 h) and the remnant pravastatin was quantified by HPLC.

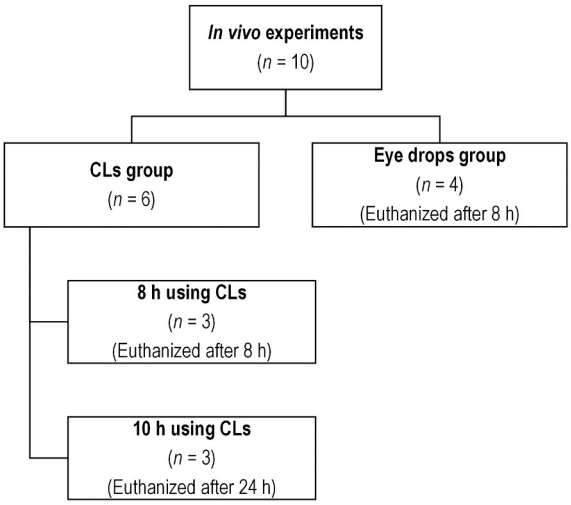

Fig. 2. Animals distribution in *in vivo* experiments.

2.9.2. *Quantification of pravastatin in tear fluid*

The Schirmer test strips were placed in 2 mL Eppendorf tubes with 200 μL of SLF for 12 h at 4 °C. For protein denaturation, the samples were vortexed for 1 min, and the strips were removed from the tubes. Then, SLF solution was heated at 98 °C for 2 min, cooled in ice for 10 min, and centrifuged at 13,000 rpm for 10 min at 25 °C [54]. Finally, the supernatants were collected and stored at −20 °C until HPLC analysis (as described in Section 2.7). In preliminary tests, this protein denaturation method was shown to reproducibly recover >95% pravastatin present in the samples.

In vitro-in vivo correlations (IVIVC) were attempted through Levy plot analysis, where the X-axis was reported as the percentage of drug released *in vitro* at a certain time, and the Y-axis the percentage of drug released in the tear fluid at the same time estimated as follows [55].

$$\text{Pravastatin } \textit{released in vivo } (\%) = (\text{AUC}_{0-t}/\text{AUC}_{0-\text{last}}) \times 100\% \quad (4)$$

Regression analysis was carried out using SigmaPlot for Windows v.14 software (Systat Sofware Inc., Germany).

2.9.3. *Quantification of pravastatin in ocular tissues*

All the rabbits were euthanized by intravenous administration of 0.75 mL/Kg of propofol and 0.5 mL/Kg of pentobarbital sodium (approx. 2 mL, Exagon 400 mg/mL). Following euthanization, aqueous humour was directly extracted from the anterior chamber using a needle and stored at 4 °C until being processed for protein denaturation. Then, the eyes were enucleated and immediately stored at −80 °C until tissue dissection, when cornea, sclera, crystalline lens, vitreous humour, and retina were weighed and separately placed in Eppendorf tubes. SLF was added to cornea (500 μL), crystalline (500 μL), sclera (800 μL) and retina (200 μL). The tissues remained immersed in SLF for 12 h at 4 °C, and then the protein denaturation process was performed as previously described. The supernatant was collected and stored at −20 °C until UPLC analysis. Before UPLC analysis all the samples were centrifuged at 5000 rpm, 4 °C for 10 min. UPLC analysis was performed on a Waters Acquity UPLC H-Class coupled with a Xevo TQD MS System. The chromatographic separation was performed on a HypersilGOLD C18 (Thermo-Fisher, 1.9 μm, 2.1 × 50 mm) column with a column temperature of 35 °C, a flow rate of 0.6 mL/min, and a mobile phase containing 0.1% formic acid/water (A) and 0.1% formic acid/acetonitrile (B). The gradient was programmed as follows: 0–0.1 min 5% B, 0.1–1.0 min 5–100% B, 1.0–2.0 min 100% B, 2.0–2.1 min 100–95% B, and 2.1–2.5 min 5% B. Electrospray ionization (ESI) was run in positive mode with a source temperature of 150 °C and a desolvation temperature of 500 °C.

Capillary voltage was set to 3 kV and the cone voltage was set to 45 V. Desolvation gas flow was 900 L/h and cone gas flow was set to 50 L/h. Pravastatin was monitored in selected ion recording (SIR) mode using the *m/z* of 447.101.

2.10. Statistical analysis

Statistical analysis was performed using Statgraphics Centurion 18 v. 18.1.13 (Statgraphics Technologies, Inc., Warrenton, VA, USA). The descriptive data were presented as mean ± standard deviation. One-way analysis of variance (ANOVA) followed by Multiple Range Test was carried out. The level of significance was 0.05.

3. Results and discussion

3.1. Hydrogels synthesis and characterization

Hydrogels were synthesized combining HEMA with EGPEM and APMA searching for a good balance between solvent uptake, light transmission and mechanical properties, and binding affinity for statins. APMA was chosen as functional monomer able to mimic cationic amino acids involved in the binding site of HMG-CoA reductase [56]. Incorporation of EGPEM was proposed for hydrophobic interactions with the benzyl group of pravastatin sodium enhancing drug binding through π–π stacking [39]. EGPEM and APMA dissolved quickly in HEMA solution at concentrations of 200 and 40 mM, respectively. The hydrogels were coded as ExAy, where x referred to the concentration of EGPEM in mM, and y referred to APMA concentration in mM in the monomers mixture.

Dried hydrogels swelled quite fast after being immersed in SLF, achieving the solvent uptake plateau in 1 h (Fig. S2A in Supplementary Material). Hydrogels prepared with the hydrophobic monomer EGPEM showed lower water uptake (44.05 ± 0.40% for E200A0) compared to those bearing only APMA (52.91 ± 1.97% for E0A0) ($p < 0.05$). APMA did not alter the swelling of HEMA hydrogels. EGPEM-bearing hydrogels also showed greater water contact angles when tested both in the dried and wet states (Table S1 in Supplementary Material); nevertheless, in all cases the contact angles were below 90° and the hydrogels can be considered to have hydrophilic surface. NaCl permeability, calculated as recorded in Fig. S1 (Supplementary Material) ranked in the order E0A40 ($8.3{\cdot}10^{-6}$ cm/s) > E0A0 ($7.8{\cdot}10^{-6}$ cm/s) > E200A0 ($5.7{\cdot}10^{-6}$ cm/s) > E200A40 ($3.5{\cdot}10^{-6}$ cm/s). The higher values corresponded to the most hydrophilic hydrogels in good agreement with previous reports and in the range typical of CLs [57,58].

For all compositions, light transmission of wet hydrogels was close to 90% in the visible range (Fig. S2B in Supplementary Material) fulfilling the requirements for CLs. Representative optical images of discs and CLs are shown in Fig. S3 (Supplementary Material). The elastic modulus of the hydrogels ranged between 0.65 and 0.79 MPa (Fig. S4 in Supplementary Material); E0A40 hydrogel presented a significantly lower value compared to the other hydrogels ($p < 0.05$). Nevertheless, the obtained values were for all hydrogels in the range of those typical for HEMA-based CLs (0.2–2.0 MPa) [59].

3.2. Pravastatin loading and in vitro release

Pravastatin loading was carried out by immersing the dried discs in pravastatin solution (0.1 mg/mL in water) for 48 h at room temperature. Loading of pravastatin during CL synthesis was discarded due to the poor solubility of the drug in the monomers mixture and the potential loss of a fraction of the incorporated drug during the required washing. Control E0A0 hydrogel loaded a small amount of pravastatin (0.42 ± 0.22 mg/g, Fig. 3A). Incorporation of EGPEM monomer (E200A0 hydrogel) did not significantly improve the affinity for pravastatin (0.32 ± 0.17 mg/g; $p > 0.05$). Differently, the copolymerization of HEMA with APMA monomer (E200A40 and E0A40 hydrogels) remarkably increased the amount of pravastatin loaded (7.26 ± 0.59 and 6.70 ± 0.20 mg/g, respectively; $p < 0.05$). The $K_{N/W}$ values recorded for APMA-containing hydrogels (66.44 ± 2.30 for E0A40 and 72.17 ± 6.78 for E200A40) were about twenty-fold higher than those recorded for control hydrogels (3.70 ± 2.58 for E0A0) and hydrogels prepared with EGPEM solely (2.75 ± 1.99 for E200A0) ($p < 0.05$). Compared to previous reports on atorvastatin [39], $K_{N/W}$ values were lower for pravastatin, which may be related to the higher hydrophilicity of the latter.

When transferred to SLF, APMA hydrogels released higher amounts of pravastatin than non-functionalized (E0A0) and EGPEM (E200A0) hydrogels (Fig. 3B). Comparing both APMA hydrogels, E200A40 presented slower release rate in the first hours, but the total amount of pravastatin released after 120 h was higher (7.84 ± 0.66 mg/g) compared to E0A40 hydrogel (7.07 ± 0.45 mg/g). The slower release rate recorded for E200A40 in the first hours may be related to the higher $K_{N/W}$ and pointed out to the role of the drug-EGPEM hydrophobic interactions in sustaining the release of the drug. These findings also suggest that both APMA and EGPEM are needed for resembling the multiple-point redundant interactions of the physiological receptor

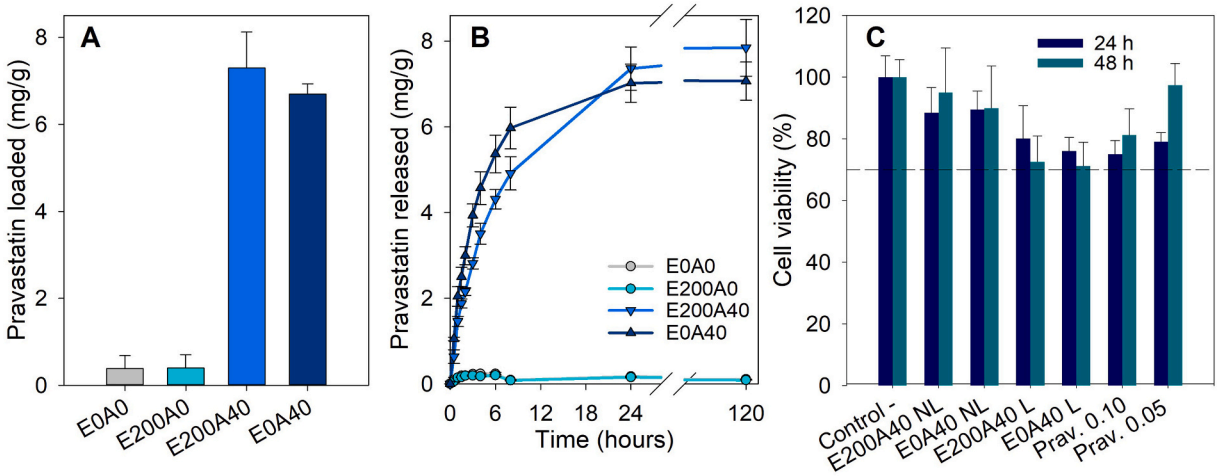

Fig. 3. (A) Pravastatin loaded by the hydrogel discs (0.3 mm thickness) after 48 h of soaking in the drug solution (0.1 mg/mL in water) at room temperature under oscillatory movement (180 osc/min); (B) release profiles from pravastatin-loaded discs in SLF at 37 °C under oscillatory movement (180 osc/min); and (C) Balb/3T3 cells viability determined by CCK-8 assay after 24 and 48 h direct exposure to non-loaded (NL) and pravastatin-loaded (L) hydrogels (E200A40 and E0A40) and two pravastatin solutions (Prav. 0.10 and 0.05 mg/mL in water). Negative control (C-): cells cultured in the absence of any treatment. Dashed line corresponds to 70% cell viability. Hydrogel codes as in Table 1 ($n = 4$; mean values and standard deviations).

[60,61]. Subsequent studies were carried out with both types of hydrogels containing APMA (E0A40 and E200A40).

3.3. Cytocompatibility and HET-CAM

Cell viability tests were performed using sterilized non-loaded and pravastatin-loaded hydrogels against Balb/3T3 fibroblasts, which is one of the most sensitive cell lines for biomaterials testing [62]. Two solutions with different concentration in pravastatin were also evaluated. After 24 h of incubation, cell viability was 88.5 ± 8.2% and 89.6 ± 6.0% for non-loaded E200A40 and E0A40 hydrogels, and 80.2 ± 10.6% and 76.1 ± 4.4% for pravastatin-loaded hydrogels, respectively (Fig. 3C). After 48 h of incubation cell viability increased for non-loaded hydrogels and slightly decreased for pravastatin-loaded ones (72.5 ± 8.4% and 71.3 ± 7.7% for E200A40 and E0A40, respectively); statistically significant differences compared to control hydrogels ($p < 0.05$). Pravastatin solution of the highest concentration tested (0.1 mg/mL) caused similar decrease in cell viability. Differently and in good agreement with previous reports, pravastatin 0.05 mg/mL was highly cytocompatible as also observed for L6 fibroblasts [63]. In addition, it should be noted that *in vitro* cell studies do not reflect tear fluid renovation and drainage, which would reduce the contact time between pravastatin released from the hydrogels and ocular surface. Overall, all hydrogels could be considered as non-cytotoxic [64].

The Hen's Egg Test on the Chorioallantoic Membrane (HET-CAM) assay was used as a preliminary test to evaluate the compatibility of the synthetized hydrogels with the ocular surface. The vascularized CAM tissue of an embryonated hen's eggs can provide information similar to the vascularized mucosal tissues of the eye, such as the conjunctiva [65]. After 5 min in contact with the CAM, pravastatin-loaded hydrogels and pravastatin solution (300 μL, 0.1 mg/mL in water) did not trigger haemorrhage, vascular lysis or coagulation of CAM vessels, and could be considered as non-irritating for the ocular surface (Fig. S5 in Supplementary Material). As expected, the positive control (NaOH 0.1 N) registered an IS of 19.24.

3.4. Effects of sterilization and light exposition on drug stability and release

Feasibility of sterilization and loading of the hydrogels in one single step was also evaluated. Firstly, the effect of SH and HHP sterilization on pravastatin solutions was tested. Pravastatin stability was compromised after exposition to 121 °C for 1 h and 1 bar originating degradation products at 3.9 min and 6.8 min (Fig. S6 in Supplementary Material). Contrarily, HHP sterilization (70 °C for 10 min and 600 MPa) did not trigger degradation, and the peak area at 5.15 min presented a variation lower than 5.5% compared to that of freshly prepared drug solution. As previously verified, degradation of pravastatin may be dramatically accelerated as temperature increases [66]. Thus, heating up to 70 °C could be pointed out as safe for pravastatin.

Sterilization tests were also carried out with hydrogel discs previously soaked in 10 mL of pravastatin solution (0.1 mg/mL) for 48 h. The hydrogels sterilized applying SH contained lower amount of drug than the non-sterilized counterparts, especially E0A40 hydrogel ($p < 0.05$) (Fig. 4 A). Importantly, the hydrogels sterilized by HHP loaded amounts of pravastatin similar to those loaded by non-sterilized hydrogels. In good agreement, the amount of pravastatin released significantly decreased for hydrogels sterilized by SH ($p < 0.05$) (Fig. 4B). Consequently, HHP was chosen for subsequent one-pot loading and sterilization of CLs.

To gain further inside into drug stability, pravastatin solutions were exposed to white light mimicking the daylight conditions in the time frame of the 6–8 h of use of daily disposable CLs, and possible light-induced degradation was evaluated. HPLC chromatograms recorded before and after 6 h of exposure were similar (Fig. S7 in Supplementary Material) with changes in peak area below 2% for replicated tests ($n = 3$), which indicated that pravastatin did not suffer degradation under light exposition. As previously observed, pravastatin is quite stable under sunlight conditions [67], which is an advantage for incorporation into CLs.

3.5. Effects of SLF volume and proteins on in vitro drug release profiles

The *in vitro* release profiles of sterilized curved E200A40 CLs (0.1 mm of thickness) were investigated under six different conditions: two volume levels (2 and 10 mL) and three protein conditions (no protein, lysozyme, or albumin). In this work, the main tear fluid proteins albumin and lysozyme were tested at a fix concentration of 2.68 mg/mL, which was considered as biorelevant [68]. Dried CLs (E200A40 formulation) were immersed in pravastatin solution (0.1 mg/mL) and sterilized by HHP (as described in section 2.8). Then, the pravastatin-loaded CLs were rinsed with SLF and immersed in the release medium (Fig. 4C).

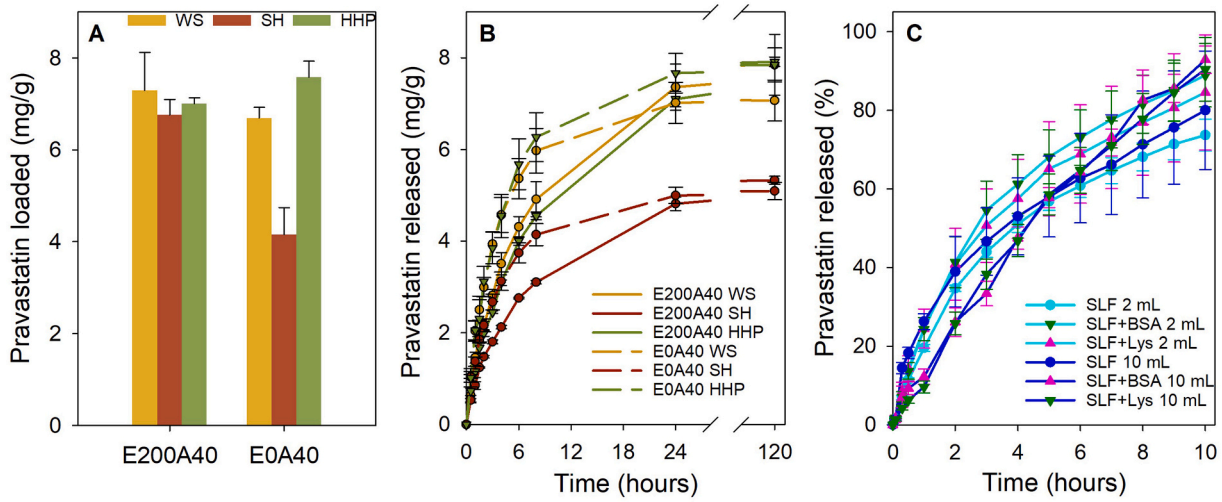

Fig. 4. (A) Pravastatin loaded by E200A40 and E0A40 hydrogels when they were sterilized in drug solution by means of steam heat (SH) or high hydrostatic pressure (HHP), compared to non-sterilized hydrogels (WS); (B) pravastatin release profiles in 10 mL of SLF from E200A40 and E0A40 hydrogels that had not being sterilized (WS) or that were sterilized during loading (immersed in drug solution); and (C) pravastatin release profiles from E200A40 CLs (previously sterilized by HHP) in 2 or 10 mL of SLF without and with incorporation of lysozyme (Lys) and bovine serum albumin (BSA). Hydrogel codes as in Table 1 ($n = 4$; mean values and standard deviations).

The amounts of drug released in 10 mL of SLF from 0.3 mm thickness E200A40 hydrogels and from 0.1 mm thickness curved CLs of the same composition after HHP sterilization were similar ($p > 0.05$). This finding revealed that the hydrogel format (in the disc-CL range evaluated) did not impact on drug release.

Pravastatin release in 2 mL of SLF was slightly slower than in 10 mL SLF, but the profiles run in parallel and no statistical differences could be detected due to the data variability. For 2 mL experiment, the incorporation of lysozyme and BSA proteins accelerated drug release, and the percentage released in the 8 to 10 h was statistically higher than in the absence of proteins ($p < 0.05$). Differently, lysozyme and BSA decreased release rate in 10 mL volume in the first 4 h but once again the percentage released in the 8 to 10 h was statistically higher than in the absence of proteins ($p < 0.05$).

As evidenced in a previous comprehensive report, the volume of the *in vitro* release medium may significantly affect drug release from CLs [33]. Since the CL is not inert against the drug, *i.e.* there exists an affinity, the volume of the release medium determines the concentration of drug outside the hydrogel, which affects to the release-rebinding equilibrium. When the loaded hydrogel is exposed to the release medium, the release is trigged by the drug concentration gradient between inside and outside the hydrogel. As more drug molecules accumulate in the release medium, hydrogels with high affinity for the drug, *i.e.* high $K_{N/W}$, may stop the release [60,69]. The drug binding interactions counteract the release, and an equilibrium is observed when the number of drug molecules that abandon the network is similar to the number that is rebound by the hydrogel. Only under infinite dilution rebinding does not occur. Therefore, in any finite volume the equilibrium may be reached, and false plateaus or delays in the release may be observed. Nevertheless, this affinity-driven controlled release phenomenon gains more relevance as the volume of the release medium decreases and the $K_{N/W}$ increases. The high solubility of pravastatin and intermediate values of $K_{N/W}$ indicated that pravastatin affinity for water is still quite high, which may explain the small effect of the volume on the percentage of pravastatin release.

Also, drug release from CLs could be affected by the presence of proteins, lipids, and mucin present in the tear film [34]. Interestingly, in this study, the incorporation of lysozyme and BSA in 2 mL volume slightly increased pravastatin release at all time points, while for 10 mL volume a change in the release profile, first slower and then faster, was observed (Fig. 4C). Lysozyme (pI 11.0) and BSA (pI 4.7) are positively and negatively charged, respectively, in SLF. Therefore, the likelihood of that their effect is related to ionic interactions with the drug or the hydrogel is low. In previous studies with a hydrophobic drug model (Rose Bengal dye), these same proteins were shown to accelerate the release, which could be related to hydrophobic interactions between the drug and the protein, promoting the extraction from the hydrogel [36]. Pravastatin sodium is a hydrophilic drug and the fraction unbound in plasma has been reported to be 0.485, which means that pravastatin is not a highly bound protein drug [70]. Also, the experimental protocol applied to denature the protein before drug quantification in the HPLC was demonstrated to recover >95% drug from the samples, which ensured that the decrease in the release was not due to losses of drug due to protein binding.

Slower release rate in artificial tear solution containing proteins and lipids was observed for moxifloxacin from a variety of CLs, compared to simple PBS [71]. As previously reported for other HEMA hydrogels [72], deposition of albumin and lysozyme on the tested CLs was very low and not measurable. Thus, although the formation of a thin layer of proteins on the CL surface that may act as an additional barrier for drug diffusion could not be discarded, its effect might be more relevant in the first hours after immersion of the discs in 10 mL medium (more total amount of proteins) due to the Voomer effect [73]. This might explain the initial slower release and also the subsequent faster release as the adsorbed proteins detach and may drag some drug molecules with them.

3.6. Ex vivo corneal and scleral permeability

Pravastatin diffusion tests from E200A40 and E0A40 hydrogels through cornea and sclera were evaluated *ex vivo* using porcine tissues. The vertical Franz cell may simulate the drug flux from the exterior of the eye to the aqueous or vitreous humour. As a control, the donor chamber was filled with a pravastatin solution (128 μg/mL) that provided an amount of pravastatin similar to the maximum amount of drug released from the hydrogels in 6 h.

After 6 h of experiment the concentration of pravastatin in the donor chamber in contact with cornea and sclera was significantly lower for both hydrogels compared to the drug solution (Fig. 5A; $p < 0.05$). No differences were found between the hydrogels.

The amount of pravastatin accumulated in cornea was significantly lower than in sclera (Fig. 5B; $p < 0.05$), but for a given tissue no differences were found among the hydrogels and the solution. This means that pravastatin released from the hydrogels during 6 h could diffuse into the tissues in a similar amount than when supplied as a solution, in spite of that in the case of the solution the entire dose was placed into contact with the cornea or sclera tissue since the very beginning of the experiment.

Pravastatin permeated through sclera was detected in the receptor chamber after two hours of contact with pravastatin solution and after three hours for E200A40 and E0A40 hydrogels (Fig. 5C). For porcine cornea tissue, the amount of pravastatin in the receptor chamber was below the HPLC quantification limit. This means that pravastatin mainly accumulated into the cornea in the time frame of the experiment. Generally, a poor penetration across the cornea was observed for more hydrophilic and larger molecules [74]. Pravastatin presents greater hydrophilicity than other statins (log $P = -0.23$) which could explain the higher sclera permeability observed. Very recently, *ex vivo* cornea and sclera permeability studies revealed that atorvastatin mainly accumulated into cornea and sclera tissues but did not progress further [39]. Due to its lipophilicity (log $P = 5.39$), atorvastatin could present higher cornea permeability, but this effect may have been thwarted by the higher molecular weight (558.64 g/mol).

In the case of sclera, flux (J) and apparent permeability coefficient (P_{app}) of pravastatin ranked in the order: E200A40 < E0A40 < pravastatin solution (Table 2). These values agreed with those previously reported for other drugs such as transferulic acid (0.035 to 0.115 μg/cm^2·h; 5.4 to 11.5·10^{-6} cm/s) and valaciclovir (0.42 to 4.23 μg/cm^2·h; 9.75 to 11.37·10^{-6} cm/s) when delivered from drug-eluting CLs [46,51].

3.7. Anti-inflammatory activity

Once pravastatin was demonstrated to be able to penetrate in the eye structures *ex vivo*, the next sept was to elucidate the anti-inflammatory activity of drug itself and of the drug-CL combination product. Cytokines and other mediators, such as prostaglandins, play important roles in eye inflammation. Some previous studies have been focused on the anti-inflammatory effects of statins, but results were not homogeneous [75–77]. McFarland et al. [77] compared the effects of the six statins (including pravastatin) on PMA differentiated THP-1 cells and using LPS to induce inflammatory conditions. All statins significantly reduced LPS-induced IL-1β and TNF-α release and also decreased prostaglandin E2 (PGE2) levels. Loppnow et al. [76] showed that pravastatin reduced the IL-6 production by 60% in human vascular smooth muscle cells (SMC) and human mononuclear cells (MNC). Conversely, Bessler et al. [75] found that the IL-6 production in human peripheral blood mononuclear cells was not affected by pravastatin.

In the present study, the secretion of tumor necrosis factor alpha (TNF-α) and interleukin-6 (IL-6), two pro-inflammatory cytokines, was examined by stimulation of macrophages with LPS. The macrophages were previously treated with non-loaded and pravastatin-loaded E200A40 hydrogels or pravastatin solutions (Fig. 6). A statistically significant reduction in TNF-α secretion ($p < 0.05$) was observed for

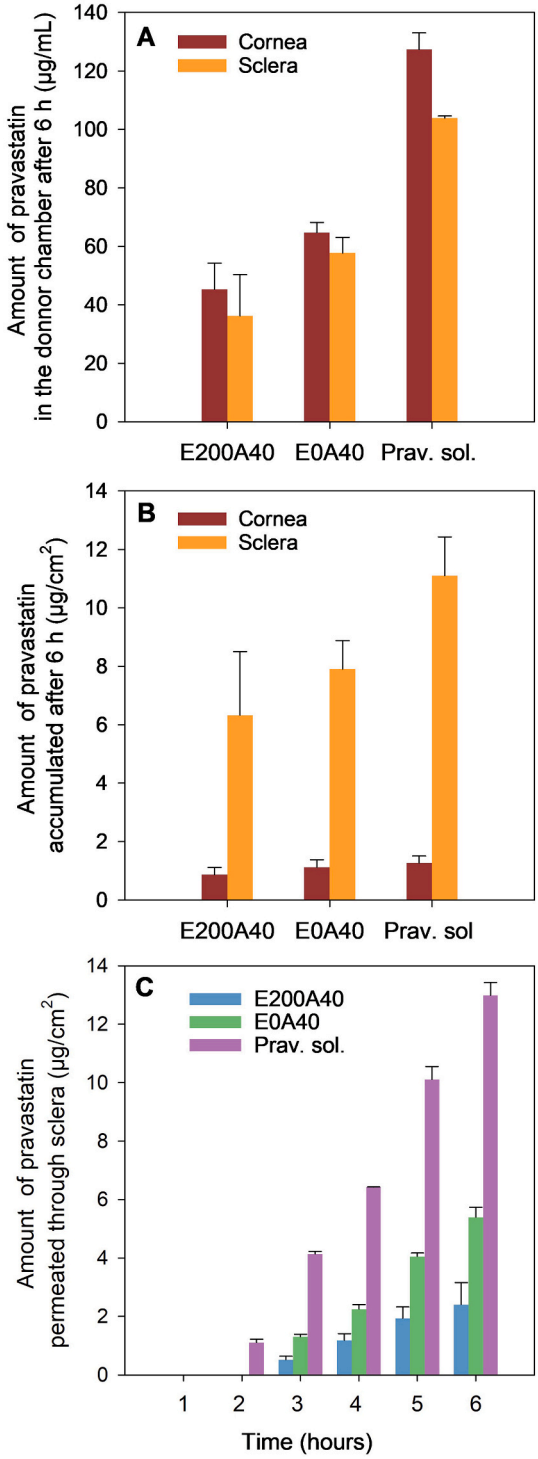

Fig. 5. (A) Amounts of pravastatin in the donor chamber, (B) amounts accumulated in cornea and sclera tissues, and (C) amounts permeated through porcine sclera after 6 h of contact with drug-loaded hydrogels (E200A40 and E0A40) and pravastatin solution (128 µg/mL, 1 mL). Codes as in Table 1 ($n = 3$; mean values and standard deviations).

pravastatin-loaded E200A40 hydrogels compared to the non-loaded hydrogels (Fig. 6A). All tested pravastatin solutions (0.1, 1, 10 µM) caused a similar decrease in the secretion of TNF-α, and no significant differences were observed for the different concentrations ($p > 0.05$). Differently, in the case of IL-6, no significant decrease was recorded, and no differences were observed ($p > 0.05$) for pravastatin-loaded E200A40 hydrogels and pravastatin solutions compared to the non-loaded

Table 2
Flux (J) and apparent permeability coefficient (P_{app}) of pravastatin applied as a solution or as pravastatin-loaded E200A40 and E0A40 hydrogels onto to sclera tissue ($n = 3$) (mean value ± standard deviations).

Formulation	J (µg/(cm^2·h))	P_{app} (×10^6) (cm/s)
E200A40	0.47 ± 0.11	3.16 ± 1.85
E0A40	1.02 ± 0.05	4.92 ± 2.93
Prav. sol	2.46 ± 0.09	6.57 ± 2.72

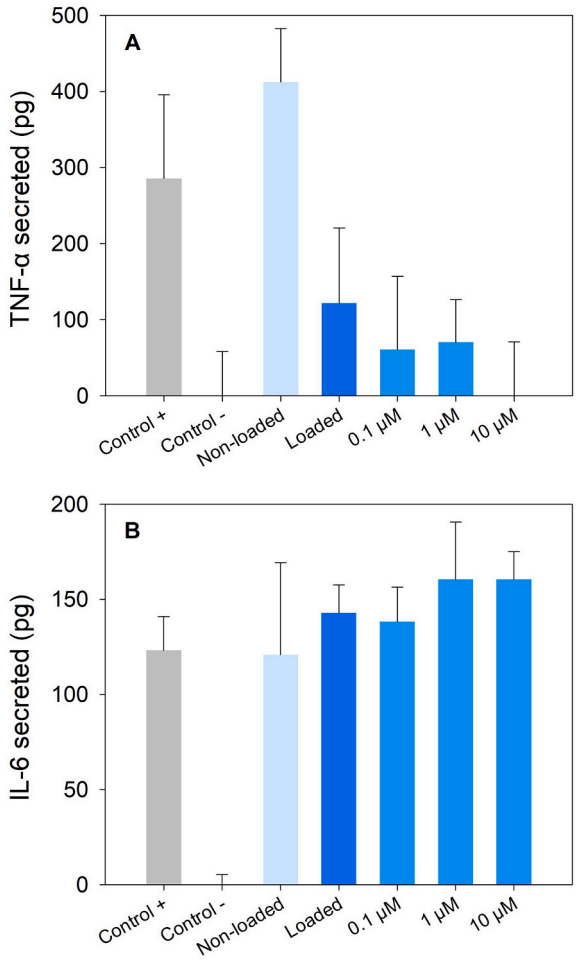

Fig. 6. Effect of non-loaded and pravastatin-loaded E200A40 discs and pravastatin sodium solutions (0.1, 1, 10 µM) on the secretion levels of (A) TNF-α and (B) IL-6 from macrophages that were previous treated with the hydrogels or pravastatin solutions followed by addition of LPS. Positive control refers to cells only stimulated with LPS; negative control refers to unstimulated cells (without LPS).

hydrogels (Fig. 6B). Overall, the obtained results point out the effectiveness of pravastatin-loaded hydrogels to decrease the secretion of TNF-α showing promising anti-inflammatory activity.

3.8. *In vivo tests*

After *in vitro*, *in ovo*, *in cell* and *ex vivo* tests were fulfilled, an *in vivo* study was planned with the double aim of (i) assess the advantages of using pravastatin-eluting CLs compared to eye drops in terms of drug levels in tear fluid and biodistribution to eye tissues (for a same drug dose), and (ii) elucidate whether *in vitro-in vivo* correlations (IVIVC) could be obtained and which *in vitro* release conditions may provide better correlations.

The *in vivo* release profiles of pravastatin in tear fluid (concentration *versus* time) after application of E200A40 CLs and eye drops (2 mg/mL of pravastatin) are shown in Fig. 7A. In the eye drops group, the maximum pravastatin concentration (C_{max}) in the rabbit tear fluid was recorded in the first 5 min (975.21 ± 456.40 μg/mL), followed by an exponential decrease, with a low drug concentration being detected after 1 h (14.88 ± 10.99 μg/mL to 9.30 ± 13.13 μg/mL at 8 h), which was found to be consistent with previous studies that demonstrated a rapid decline [52,55,78].

Pravastatin-loaded CLs led to a smoother concentration curve and a sustained release over a period of 10 h, which demonstrated much less variability in the concentration of pravastatin in tear fluid and a significant improvement in mean residence time of pravastatin (Table 3). The C_{max} was found to be 177.5 ± 116.8 μg/mL after 30 min of CL wearing. No burst release was observed. Only in the first 5 min, pravastatin concentration in tear fluid was higher for the eye drop group than for the CL group ($p < 0.05$). No statistically significant differences were recorded at 15 and 30 min. After that, the concentrations recorded in the CL group were higher than those provided by the eye drops in the first 7 h of wearing (with the exception of time point 6 h, which were not significantly different). When wearing drug-loaded CLs, pravastatin diffused through the CL matrix and gradually entered the post-lens tear film prolonging the retention in the precorneal area. Previous studies also evidenced that drug-eluting CLs can improve drug retention in comparison with eye drops. For example, in New Zealand white rabbits, the MRT of ketotifen delivered from non-imprinted CLs wore for an entire day was found to be 3.4 h compared to 0.25 h for eye drops [61]. Also, CLs loaded with timolol during synthesis increased the mean residence time from 0.33 h for eye drops to 26.27 h for CLs wore for 5 days [55]. In our case, pravastatin-loaded CLs were intended to be daily disposable and, therefore, the release was aimed to be completed in the common half a day time frame of CL wearing. Indeed, the amounts of pravastatin remnant inside the CLs after 8 h and 10 h wearing were 7.5 ± 4.2 μg and 2.8 ± 1.6 μg, respectively, which indicated that >90% drug was released in the first 8 h of wearing. Thus, when the CLs were taken out, environmental impact due to waste of drug was not expected. Pravastatin-loaded CLs provided >2-fold increase in $AUC_{0\text{-}8h}$ and almost triplicate the MRT compared to the eye drops, for the same dose administered of 100 μg. MRT values of 2.82 h recorded for pravastatin-loaded CLs were significantly larger than those recorded for timolol (~ 0.3 h) [53] and puerarin (1.3 h) [79] using HEMA-based CLs.

Table 3
Pharmacokinetic parameters obtained from the pravastatin concentration-time profiles in tear fluid for an equivalent dose of 100 μg administered as CL (n = 6) or eye drop (n = 4) (mean values and standard deviations).

Formulation	C_{max} (μg/mL)	t_{max} (h)	$AUC_{0\text{-}8h}$ (μg/mL·h)	$AUMC_{0\text{-}8h}$ (μg·h/mL·h)	MRT (h)
E200A40 CLs	177.5 ± 116.8	0.50	573.5 ± 193.1	1637.3 ± 637.6	2.82 ± 0.24
Eye drops	975.2 ± 456.4	0.08	267.6 ± 94.3	365.9 ± 319.2	1.17 ± 0.89

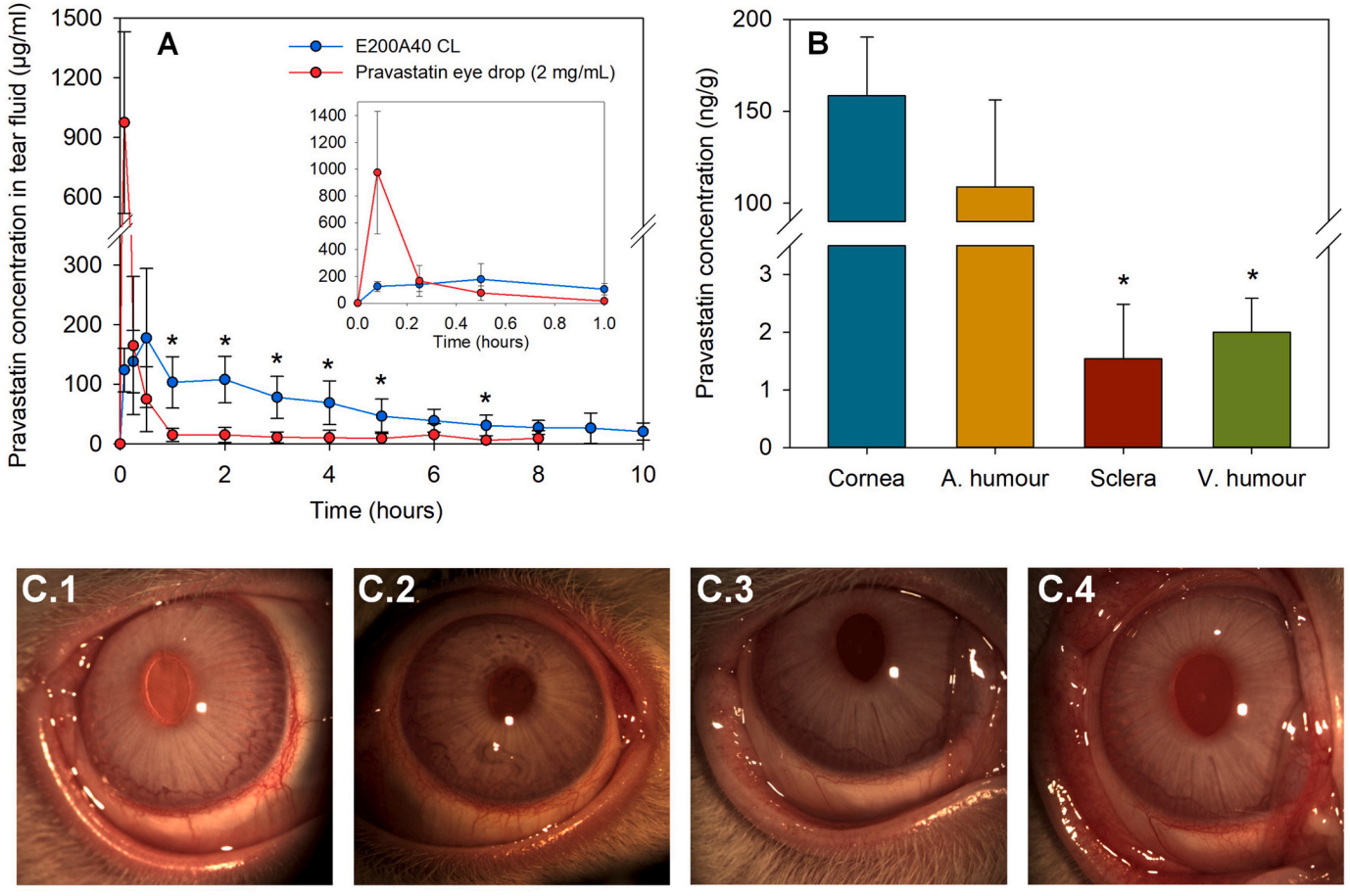

Fig. 7. (A) Pravastatin concentration in the tear fluid during E200A40 CL wearing (n = 6 for 8 h and n = 3 for 9 and 10 h) and after a single instillation of pravastatin eye drops (50 μL, 2 mg/mL, n = 4) (mean values and standard deviations; *CLs provided statistically significant higher concentrations than eye drops; $p < 0.05$); (B) pravastatin accumulated in various ocular tissues after 8 h of CL wear (n = 3; * statistically different from the amount of pravastatin accumulated in the cornea; $p < 0.05$); and (C) slit-lamp images of rabbits' eyes without CLs (C.1) before and (C.2) after 8 h of wearing E200A40 CLs and (C.3) before and (C.4) after administration of a single eye drop (2 mg/mL).

The left eye of the rabbits served as a control, and no pravastatin was detected in tear fluid of left eye during treatment of the right eye either with CLs or eye drops. Also, no traces of pravastatin were detected in the tissues of the left eye. Therefore, systemic absorption could be considered as unlikely.

Biodistribution of pravastatin in the anterior and posterior segments of the eye was investigated after 8 h of CL wearing and eye drop instillation. The amount of pravastatin in eye tissues was also quantified 14 h later of removing the CLs that were wore for 10 h in order to mimic the rest period without CL, which may provide information about risk of drug accumulation. Among the ocular tissues evaluated (cornea, crystalline lens, sclera, retina, aqueous humour and vitreous humour), pravastatin was detected in cornea, sclera, aqueous humour and vitreous humour after 8 h of CL wearing (Fig. 7B). Pravastatin was not detected in rabbits' left eye (control) neither in the eye drops group. A preferential biodistribution of pravastatin was observed in the anterior segment, which provided the highest accumulation in the cornea (158.46 ± 31.8 ng/g) and aqueous humour (108.73 ± 47.48 ng/g). CLs also facilitated pravastatin biodistribution and accumulation in the posterior segment, including sclera (1.53 ± 0.59 ng/g) and vitreous humour (2.00 ± 0.59 ng/g). It should be noted that no pravastatin was detected in eye tissues of rabbits that wore CLs for 10 h and remained 14 h more without CLs, which avoids risks of drug accumulation after successive applications. The rabbit model, although widely used, may have the limitation of lower blinking rate, and thus the release might be somehow faster when CL are applied to human eyes [80,81].

Slit-lamp images were collected to evaluate a possible ocular irritation after 8 h of wearing pravastatin-loaded CLs or eye drops administration (Fig. 7C). No signs of ocular irritation were observed in any rabbit. Hence, pravastatin-loaded CLs showed good compatibility and safety to the rabbits' eyes as revealed in previous designed and optimized HEMA-based CLs.

3.8.1. *In vitro-in vivo correlations*

Comparison between *in vivo* and *in vitro* release profiles in 2 and 10 mL of SLF are shown in Fig. S8 (Supplementary Material). The *in vivo* data showed similar percentages of drug released in the first hours but then accelerated compared to the *in vitro* release. Levy plots (Fig. 8A and B) were used to investigate *in vitro-in vivo* correlations (IVIVC). The regression was not forced to pass through the origin in order to see better the deviations at short times. *In vitro* release tests carried out in 2 mL led to Levy plots with correlation coefficient (r^2) values closer to 1 compared to the Levy plots obtained for 10 mL.

For 2 mL SLF (Fig. 8A), the intercepts at the origin were in the −5 to −6 range disregarding the presence or absence of proteins and the slopes were 1.476 (s.e. 0.030), 1.321 (s.e. 0.036) and 1.224 (s.e. 0.028) for medium without proteins, with BSA and with lysozyme, respectively. Thus, strong correlations but with positive deviations were observed, and the slope shifted towards 1 in the presence of proteins.

For 10 mL SLF (Fig. 8B), in the absence of proteins the intercept at the origin was −12.8, which evidenced that the percentage released *in vitro* was remarkably higher at the very beginning, and the slope was 1.536 (s.e. 0.072). In the presence of BSA and lysozyme the intercepts at the origin were in the +4 to +5 range and the slopes were 1.245 (s.e. 0.078) and 1.251 (s.e. 0.053), respectively. Thus, the presence of proteins in the *in vitro* release medium favored the goodness of the IVIVC.

4. Conclusions

CLs prepared with EGPEM and APMA as monomers that can resemble the hydrophobic and amine-based binding points of the natural receptor have been shown able to load remarkably high pravastatin amounts. Pravastatin-loaded CLs exhibited swelling capacity, light transmission and mechanical properties typical of soft CLs (thus, they may be suitable for refractive errors correction) and also sustained *in vitro* release for 10 h. Preliminary biocompatibility tests in cell cultures,

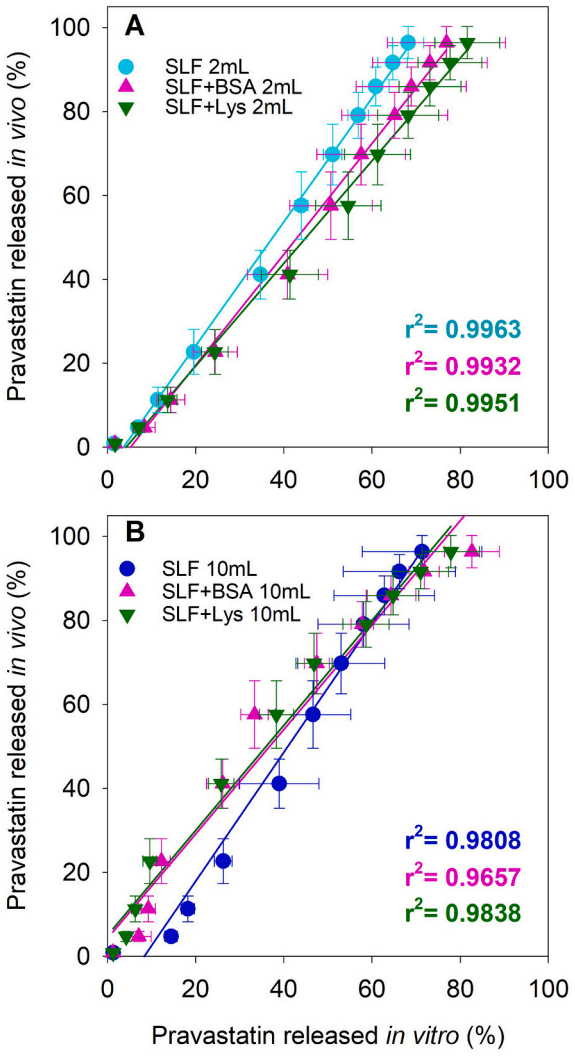

Fig. 8. Levy plots for *in vivo vs. in vitro* percentage of drug released. The *in vitro* tests were carried out in (A) 2 mL of SLF solely or with BSA or lysozyme, and (B) 10 mL of SLF solely or with BSA or lysozyme.

HET-CAM and then *in vivo* confirmed the safety of this combination product. Regarding efficacy, pravastatin released from the CLs exhibited anti-inflammatory properties and capability to penetrate and accumulate in anterior and posterior eye segments. *In vivo* tests evidenced the suitability of the developed CLs to control pravastatin release on the ocular surface, notably prolonging the permanence time in the tear fluid compared to eye drops and also facilitating drug access to aqueous humour and vitreous humour. Preliminary assessment of IVIVC revealed that, despite pravastatin is not a highly bound protein drug and the CLs have low affinity for proteins, addition of BSA or lysozyme to the release medium may affect to the *in vitro* release profiles. Indeed, more linear Levy plots and with slopes closer to 1 were recorded for *in vitro* release media containing proteins. The information gathered in the present study may serve as a first step towards the search of how a change in the performance of the CLs to regulate drug release *in vitro* may be translated to a change in the *in vivo* drug profiles.

CRediT authorship contribution statement

Ana F. Pereira-da-Mota: Software, Methodology, Validation, Formal analysis, Data curation, Investigation, Writing – original draft. **Maria Vivero-Lopez:** Methodology, Validation, Formal analysis, Data curation, Investigation. **Maria Serramito:** Methodology, Investigation.

Luis Diaz-Gomez: Methodology, Investigation. **Ana Paula Serro:** Supervision, Writing – review & editing. **Gonzalo Carracedo:** Supervision, Writing – review & editing. **Fernando Huete-Toral:** Methodology, Validation, Formal analysis, Investigation, Writing – review & editing. **Angel Concheiro:** Conceptualization, Project administration, Resources, Supervision, Funding acquisition, Writing – review & editing. **Carmen Alvarez-Lorenzo:** Methodology, Conceptualization, Project administration, Resources, Supervision, Funding acquisition, Writing – original draft, Writing – review & editing.

Declaration of Competing Interest

None.

Acknowledgments

This project was funded by the European Union's Horizon 2020 research and innovation programme under the Marie Skłodowska-Curie Actions grant agreement N° 813440 (ORBITAL–Ocular Research by Integrated Training And Learning). The work was also partially supported by MCIN [PID 2020-113881RB-I00/AEI/10.13039/501100011033], Spain, Xunta de Galicia [ED431C 2020/17], FEDER and by Fundação para a Ciência e a Tecnologia (FCT, Portugal) [UIDB/00100/2020 and PTDC/CTM-CTM/2353/2021]. M. Vivero-Lopez acknowledges Xunta de Galicia (Consellería de Cultura, Educación e Ordenación Universitaria) for a predoctoral research fellowship [ED481A-2019/120]. The authors are grateful to Mabel Loza and Cristina Val García, from BioFarma USC Group, for help with UPLC experiments.

Appendix A. Supplementary data

Supplementary data to this article can be found online at https://doi.org/10.1016/j.jconrel.2022.06.001.

References

[1] O. Bedi, V. Dhawan, P.L. Sharma, P. Kumar, Pleiotropic effects of statins: new therapeutic targets in drug design, Naunyn Schmiedeberg's Arch. Pharmacol. 389 (2016) 695–712.
[2] J.K. Liao, U. Laufs, Pleiotropic effects of statins, Annu. Rev. Pharmacol. Toxicol. 45 (2005) 89–118.
[3] K.G.J. Ooi, P. Khoo, V. Vaclavik, S.L. Watson, Statins in ophthalmology, Surv. Ophthalmol. 64 (2019) 401–432.
[4] A. Gupta, V. Gupta, S. Thapar, A. Bhansali, Lipid-lowering drug atorvastatin as an adjunct in the management of diabetic macular edema, Am J. Ophthalmol. 137 (2004) 675–682.
[5] A. Ozkiris, K. Erkilic, A. Koc, S. Mistik, Effect of atorvastatin on ocular blood flow velocities in patients with diabetic retinopathy, Br. J. Ophthalmol. 91 (2007) 69–73.
[6] Y.R. Chung, S.W. Park, S. Choi, S.W. Kim, K.Y. Moon, J.H. Kim, K. Lee, Association of statin use and hypertriglyceridemia with diabetic macular edema in patients with type 2 diabetes and diabetic retinopathy, Cardiovasc. Diabetol. 16 (2017) 4.
[7] S.F. Nielsen, B.G. Nordestgaard, Statin use before diabetes diagnosis and risk of microvascular disease: a nationwide nested matched study, Lancet Diabetes Endocrinol. 2 (2014) 894–900.
[8] International Diabetes Federation, IDF Diabetes Atlas, Available from, http://www.diabetesatlas.org/>, 2022 (Accessed on 10 February 2022).
[9] N. Sayin, Ocular complications of diabetes mellitus, World J. Diabetes 6 (2015) 92–108.
[10] S.L. Misra, G.D. Braatvedt, D.V. Patel, Impact of diabetes mellitus on the ocular surface: a review, Clin. Exp. Opthalmol. 44 (2016) 278–288.
[11] D. Gologorsky, A. Thanos, D. Vavvas, Therapeutic interventions against inflammatory and angiogenic mediators in proliferative diabetic retinopathy, Mediat. Inflamm. 2012 (2012), 629452.
[12] T.Y. Wong, C.M.G. Cheung, M. Larsen, S. Sharma, R. Simó, Diabetic retinopathy, Nat. Rev. Dis. Primers 2 (2016) 16012.
[13] K. Esposito, F. Nappo, R. Marfella, G. Giugliano, F. Giugliano, M. Ciotola, L. Quagliaro, A. Ceriello, D. Giugliano, Inflammatory cytokine concentrations are acutely increased by hyperglycemia in humans: role of oxidative stress, Circulation 106 (2002) 2067–2072.
[14] S.D. Schoenberger, S.K. Kim, J. Sheng, K.A. Rezaei, M. Lalezary, E. Cherney, Increased prostaglandin E2 (PGE2) levels in proliferative diabetic retinopathy, and correlation with VEGF and inflammatory cytokines, Invest. Ophthalmol. Vis. Sci. 53 (2012) 5906–5911.
[15] J. Zhang, G. McGwin, Association of statin use with the risk of developing diabetic retinopathy, Arch. Ophthalmol. 125 (2007) 1096–1099.
[16] E. Ioannidou, V.S. Tseriotis, K. Tziomalos, Role of lipid-lowering agents in the management of diabetic retinopathy, World J. Diabetes 8 (2017) 1–6.
[17] C. Murphy, E. Deplazes, C.G. Cranfield, A. Garcia, The role of structure and biophysical properties in the pleiotropic eects of statins, Int. J. Mol. Sci. 21 (2020) 8745.
[18] K.G.J. Ooi, D. Wakefield, F.A. Billson, S.L. Watson, Efficacy and safety of topical atorvastatin for the treatment of dry eye associated with blepharitis: a pilot study, Ophthalmic Res. 54 (2015) 26–33.
[19] C.C. Li, A. Chauhan, Modeling ophthalmic drug delivery by soaked contact lenses, Ind. Eng. Chem. Res. 45 (2006) 3718–3734.
[20] P. Dixon, T. Ghosh, K. Mondal, A. Konar, A. Chauhan, S. Hazra, Controlled delivery of pirfenidone through vitamin E-loaded contact lens ameliorates corneal inflammation, Drug Deliv. Transl. Res. 8 (2018) 1114–1126.
[21] C. Wu, P.W. Or, J.I.T. Chong, I.K.K.P. Don, C.H.C. Lee, K. Wu, M. Yu, D.C.C. Lam, Y. Yang, Extended delivery of pirfenidone with novel, soft contact lenses in vitro and in vivo, J. Ocul. Pharmacol. Ther. 37 (2021) 75–83.
[22] Johnson & Johnson News, Johnson & Johnson Vision Receives Approval in Canada for World's First and Only Drug-Releasing Contact Lens for Vision Correction and Allergic Eye Itch: ACUVUE® Theravision™ with Ketotifen, April 7, https://www.jjvision.com/press-release/johnson-johnson-vision-receives-approval-canada-worlds-first-and-only-drug-releasing, 2021.
[23] Y. Zhu, Y. Sheng, Sustained delivery of epalrestat to the retina using PEGylated solid lipid nanoparticles laden contact lens, Int. J. Pharm. 587 (2020), 119688.
[24] Y. Shikamura, Y. Yamazaki, T. Matsunaga, T. Sato, A. Ohtori, K. Tojo, Hydrogel ring for topical drug delivery to the ocular posterior segment, Curr. Eye Res. 41 (2016) 653–661.
[25] F.A. Maulvi, R.J. Patil, A.R. Desai, M.R. Shukla, R.J. Vaidya, K.M. Ranch, B. A. Vyas, S.A. Shah, D.O. Shah, Effect of gold nanoparticles on timolol uptake and its release kinetics from contact lenses: in vitro and in vivo evaluation, Acta Biomater. 86 (2019) 350–362.
[26] C. Alvarez-Lorenzo, S. Anguiano-Igea, A. Varela-García, M. Vivero-Lopez, A. Concheiro, Bioinspired hydrogels for drug-eluting contact lenses, Acta Biomater. 84 (2019) 49–62.
[27] K. Kakisu, T. Matsunaga, S. Kobayakawa, T. Sato, T. Tochikubo, Development and efficacy of a drug-releasing soft contact lens, Invest. Ophthalmol. Vis. Sci. 54 (2013) 2551–2556.
[28] T. Minami, W. Ishida, T. Kishimoto, I. Nakajima, S. Hino, R. Arai, T. Matsunaga, A. Fukushima, S. Yamagami, In vitro and in vivo performance of epinastine hydrochloride releasing contact lenses, PLoS One 14 (2019), e0210362.
[29] P. Sekar, A. Chauhan, Effect of vitamin-E integration on delivery of prostaglandin analogs from therapeutic lenses, J. Colloid Interface Sci. 539 (2019) 457–467.
[30] S.A. DiPasquale, B. Uricoli, M.C. DiCerbo, T.L. Brown, M.E. Byrne, Controlled release of multiple therapeutics from silicone hydrogel contact lenses for post-cataract/post-refractive surgery and uveitis treatment, Transl. Vis. Sci. Technol. 10 (2021) 5.
[31] S.A. DiPasquale, L.D. Wuchte, R.J. Mosley, R.M. Demarest, M.L. Voyles, M. E. Byrne, One week sustained in vivo therapeutic release and safety of novel extended-wear silicone hydrogel contact lenses, Adv. Healthc. Mater. (2021) 2101263.
[32] N. Toffoletto, B. Saramago, A.P. Serro, Therapeutic ophthalmic lenses: a review, Pharmaceutics 13 (2021) 36.
[33] A. Tieppo, A.C. Boggs, P. Pourjavad, M.E. Byrne, Analysis of release kinetics of ocular therapeutics from drug releasing contact lenses: best methods and practices to advance the field, Cont. Lens Anterior Eye 37 (2014) 305–313.
[34] A. Mahomed, J.S. Wolffsohn, B.J. Tighe, Structural design of contact lens-based drug delivery systems; in vitro and in vivo studies of ocular triggering mechanisms, Cont. Lens Anterior Eye 39 (2016) 97–105.
[35] P. Paradiso, R. Colaço, J.L.G. Mata, R. Krastev, B. Saramago, A.P. Serro, Drug release from liposome coated hydrogels for soft contact lenses: the blinking and temperature effect, J. Biomed. Mater. Res. B 105B (2017) 1799–1807.
[36] C.M. Phan, M. Shukla, H. Walther, M. Heynen, D. Suh, L. Jones, Development of an in vitro blink model for ophthalmic drug delivery, Pharmaceutics 13 (2021) 300.
[37] A. Hui, M. Willcox, In vivo studies evaluating the use of contact lenses for drug delivery, Optom. Vis. Sci. 93 (2016) 367–376.
[38] A.F. Pereira-da-Mota, C.M. Phan, A. Concheiro, L. Jones, C. Alvarez-Lorenzo, Testing drug release from medicated contact lenses: the missing link to predict in vivo performance, J. Control. Release 343 (2022) 672–702.
[39] A.F. Pereira-da-Mota, M. Vivero-Lopez, A. Topete, A.P. Serro, A. Concheiro, C. Alvarez-Lorenzo, Atorvastatin-eluting contact lenses: effects of molecular imprinting and sterilization on drug loading and release, Pharmaceutics 13 (2021) 606.
[40] K.S. Jain, M.K. Kathiravan, R.S. Somania, C.J. Shishoo, The biology and chemistry of hyperlipidemia, Bioorg. Med. Chem. 15 (2007) 4674–4699.
[41] C. Alvarez-Lorenzo, H. Hiratani, J.L. Gómez-Amoza, R. Martínez-Pacheco, C. Souto, A. Concheiro, Soft contact lenses capable of sustained delivery of timolol, J. Pharm. Sci. 91 (2002) 2182–2192.
[42] E. Kim, M. Saha, K. Ehrmann, Mechanical properties of contact lens materials, Eye Contact Lens 44 (2018) S148–S156.
[43] S.W. Kim, Y.H. Bae, T. Okano, Hydrogels: swelling, drug loading, and release, Pharm. Res. 9 (1992) 283–290.
[44] F. Alvarez-Rivera, A.P. Serro, D. Silva, A. Concheiro, C. Alvarez-Lorenzo, Hydrogels for diabetic eyes: naltrexone loading, release profiles and cornea penetration, Mater. Sci. Eng. C 105 (2019), 110092.

[45] W. Chanput, J.J. Mes, H.J. Wichers, THP-1 cell line: An in vitro cell model for immune modulation approach, Int. Immunopharmacol. 23 (2014) 37–45.
[46] A. Varela-Garcia, A. Concheiro, C. Alvarez-Lorenzo, Cytosine-functionalized bioinspired hydrogels for ocular delivery of antioxidant transferulic acid, Biomater. Sci. 8 (2020) 1171–1180.
[47] L. Wang, J. Lou, J. Cao, T. Wang, J. Liu, W. Mi, Bicarbonate Ringer's solution for early resuscitation in hemorrhagic shock rabbits, Ann. Transl. Med. 9 (2021) 462.
[48] S.K. Paliwal, R. Chauhan, V. Sharma, D.K. Majumdar, S. Paliwal, Entrapment of ketorolac tromethamine in polymeric vehicle for controlled drug delivery, Indian J. Pharm. Sci. 71 (2009) 687–691.
[49] A. Onal, O. Sagirli, Development of a selective LC method for the determination of pravastatin sodium, Chromatogr. 64 (2006) 157–162.
[50] M. Al-Ghabeish, X. Xu, Y.S. Krishnaiah, Z. Rahman, Y. Yang, M.A. Khan, Influence of drug loading and type of ointment base on the in vitro performance of acyclovir ophthalmic ointment, Int. J. Pharm. 495 (2015) 783–791.
[51] A. Varela-Garcia, A. Concheiro, C. Alvarez-Lorenzo, Soluplus micelles for acyclovir ocular delivery: formulation and cornea and sclera permeability, Int. J. Pharm. 552 (2018) 39–47.
[52] O.P. van Bijsterveld, Diagnostic tests in the sicca syndrome, Arch. Ophthalmol. 82 (1969) 10–14.
[53] H. Hiratani, A. Fujiwara, Y. Tamiya, Y. Mizutani, C. Alvarez-Lorenzo, Ocular release of timolol from molecularly imprinted soft contact lenses, Biomaterials 26 (2005) 1293–1298.
[54] E.R. Lazarowski, R.C. Boucher, T.K. Harden, Mechanisms of release of nucleotides and integration of their action as P2X- and P2Y-receptor activating molecules, Mol. Pharmacol. 64 (2003) 785–795.
[55] J. Xu, Y. Ge, R. Bu, A. Zhang, S. Feng, J. Wang, J. Gou, T. Yin, H. He, Y. Zhang, X. Tang, Co-delivery of latanoprost and timolol from micelles-laden contact lenses for the treatment of glaucoma, J. Control. Release 305 (2019) 18–28.
[56] E.S. Istvan, J. Deisenhofer, Structural mechanism for statin inhibition of HMG-CoA reductase, Science 292 (2001) 1160–1164.
[57] C.C. Peng, A. Chauhan, Ion transport in silicone hydrogel contact lenses, J. Membr. Sci. 399-400 (2012) 95–105.
[58] J. Pozuelo, V. Compañ, J.M. González-Méijome, M. González, S. Mollá, Oxygen and ionic transport in hidrogel and silicone-hydrogel contact lens materials: an experimental and theoretical study, J. Membr. Sci. 452 (2014) 62–72.
[59] C.S.A. Musgrave, F. Fang, Contact lens materials: a materials science perspective, Materials 12 (2019) 261.
[60] A. Ribeiro, F. Veiga, D. Santos, J.J. Torres-Labandeira, A. Concheiro, C. Alvarez-Lorenzo, Bioinspired imprinted pHEMA-hydrogels for ocular delivery of carbonic anhydrase inhibitor drugs, Biomacromolecules 12 (2011) 701–709.
[61] A. Tieppo, C.J. White, A.C. Paine, M.L. Voyles, M.K. McBride, M.E. Byrne, Sustained in vivo release from imprinted therapeutic contact lenses, J. Control. Release 157 (2012) 391–397.
[62] J.C. Wataha, C.T. Hanks, Z. Sun, Effect of cell line on in vitro metal ion cytotoxicity, Dent. Mater. 10 (1994) 156–161.
[63] M. Itagaki, A. Takaguri, S. Kano, S. Kaneta, S. Ichihara, K. Satoh, Possible mechanisms underlying statin-induced skeletal muscle toxicity in L6 fibroblasts and in rats, J. Pharmacol. Sci. 109 (2009) 94–101.
[64] ISO 10993-5, Biological Evaluation of Medical Devices—Part 5: Tests for In Vitro Cytotoxicity, Available online, https://www.iso.org/obp/ui/#iso:std:iso:10993:-5:ed-3:v1:en, 2009 (accessed on 11 February 2022).
[65] A.S. Kishore, P.A. Surekha, P.V.R. Sekhar, A. Srinivas, P. Balakrishna Murthy, Hen egg chorioallantoic membrane bioassay: an in vitro alternative to draize eye irritation test for pesticide screening, Int. J. Toxicol. 27 (2008) 449–453.
[66] S. Brain-Isasi, C. Requena, A. Álvarez-Lueje, Stability study of pravastatin under hydrolytic conditions assessed by HPLC, J. Chil. Chem. Soc. 53 (2008) 4.
[67] A. Ahmad, B.P. Panda, M.A. Mujeeb, A validated stability-indicating method for simultaneous analysis of mevastatin and pravastatin in fermentation broth during bioconversion by Actinomadura macra, Acta Chromatogr. 23 (2011) 121–131.
[68] R.C. Marques, M. Loebenberg, M. Almukainzi, Simulated biological fluids with possible application in dissolution testing, Dissol. Technol. 18 (2011) 15–28.
[69] B. Blanco-Fernández, M. López-Viota, A. Concheiro, C. Alvarez-Lorenzo, Synergistic performance of cyclodextrin-agar hydrogels for ciprofloxacin delivery and antimicrobial effect, Carbohydr. Polym. 85 (2011) 765–774.
[70] J. Mao, U. Doshi, M. Wright, C.E.C.A. Hop, A.P. Li, Y. Chen, Prediction of the pharmacokinetics of pravastatin as an OATP substrate using plateable human hepatocytes with human plasma data and PBPK modeling, CPT Pharmacometrics Syst. Pharmacol. 7 (2018) 251–258.
[71] C. Phan, M. Bajgrowicz-Cieslak, L.N. Subbaraman, L. Jones, Release of moxifloxacin from contact lenses using an in vitro eye model: impact of artificial tear fluid composition and mechanical rubbing, TVST 5 (2016) 6.
[72] O. Moradi, H. Modarress, M. Noroozi, Experimental study of albumin and lysozyme adsorption onto acrylic acid (AA) and 2-hydroxyethyl methacrylate (HEMA) surfaces, J. Colloid Interface Sci. 271 (2004) 16–19.
[73] P. Vilaseca, K.A. Dawson, G. Franzese, Understanding and modulating the competitive surface-adsorption of proteins through coarse-grained molecular dynamics simulations, Soft Matter 9 (2013) 6978–6985.
[74] A. Subrizi, E.M. del Amo, V. Korzhikov-Vlakh, T. Tennikova, M. Ruponen, A. Urtti, Design principles of ocular drug delivery systems: importance of drug payload, release rate, and material properties, Drug Discov. Today 24 (2019) 1446–1457.
[75] H. Bessler, H. Salman, M. Bergman, R. Straussberg, M. Djaldetti, In vitro effect of statins on cytokine production and mitogen response of human peripheral blood mononuclear cells, Clin. Immunol. 117 (2005) 73–77.
[76] H. Loppnow, L. Zhang, M. Lautenschläger, L. Chen, A. Frister, A. Schlitt, N. Song, B. Hofmann, S. Rose-John, R. Silber, U. Müller-Werdan, K. Werdan, Statins potently reduce the cytokine-mediated IL-6 release in SMC/MNC cocultures, J. Cell. Mol. Med. 15 (2011) 994–1004.
[77] A.J. McFarland, A.K. Davey, S. Anoopkumar-Dukie, Statins reduce lipopolysaccharide-induced cytokine and inflammatory mediator release in an in vitro model of microglial-like cells, Mediat. Inflamm. 2017 (2017) 2582745.
[78] F.A. Maulvi, D.H. Lakdawala, A.A. Shaikh, A.R. Desai, H.H. Choksi, R.J. Vaidya, K. M. Ranch, A.R. Koli, B.A. Vyas, D.O. Shah, In vitro and in vivo evaluation of novel implantation technology in hydrogel contact lenses for controlled drug delivery, J. Control. Release 226 (2016) 47–56.
[79] J. Xu, X. Li, F. Sun, Preparation and evaluation of a contact lens vehicle for puerarin delivery, J. Biomater. Sci. Polym. Ed. 21 (2010) 271–288.
[80] D. Maurice, The effect of the low blink rate in rabbits on topical drug penetration, J. Ocul. Pharmacol. Ther. 11 (1995) 297–304.
[81] R. Galante, P. Paradiso, M.G. Moutinho, A.I. Fernandes, J.L.G. Mata, A.P.A. Matos, R. Colaço, B. Saramago, A.P. Serro, About the effect of eye blinking on drug release from pHEMA-based hydrogels: an in vitro study, J. Biomater. Sci. Polym. Ed. 26 (2015) 235–251.